Impact of IASI thermal infrared measurements on global ozone reanalyses. Reply to referee # 1

Emanuele Emili[1] and Mohammad El Aabaribaoune[1]

[1]CECI, Université de Toulouse, Cerfacs, CNRS, Toulouse, France

Correspondence: Emili (emili@cerfacs.fr)

1 Reply to general comments

We would like to thank the reviewer for his comments, which helped to improve significantly the manuscript. Detailed replies to his comments follow:

1. *The authors now mostly focus on evaluations of zonal mean concentration at five latitude bands (Figs. 2.3), or as zonal mean (Figure 5). In addition it would be interesting to see the performance of the assimilation system for more regional variations, e.g. by plotting presenting evaluations as in Figs 2/3 specific for certain regions (e.g. Europe), or presenting the data as in Figure 5, but (for instance) showing a lot/lat plot averaged over DJF and JJA, at selected altitude levels.*

   Answer: We included in the revised manuscript global maps of Tropospheric Ozone Column (1000 hPa - tropopause), as defined in Ziemke et al. (2006), averaged on DJF, MAM, JJA and SON months (Fig. 1, 2, 3, 4 in this document respectively). These plots allow now to evaluate the geographical distribution of tropospheric ozone from the different models with respect to OMI-MLS retrievals. The same tropopause level (NCEP climatology) used to compute OMI-MLS retrievals have been used to compute the model columns, as already done previously to compute Fig. 4 of the original manuscript. A new section has been added in the revised manuscript (after Sec. 5.1) to discuss the new figures, which is reported below:

   Comparison of tropospheric ozone columns

   Ozonesondes are valuable measurements to evaluate modeled ozone profiles in the troposphere but their geographical distribution is uneven and their number is relatively small in the tropical and Southern Hemisphere (SH) latitudes. OMI-MLS retrievals (Ziemke et al., 2006, 2011) provide a satellite-based estimation of the TOC that can be used to evaluate models geographical variability in tropical and mid-latitude regions. Hence, OMI-MLS TOC permits to evaluate models in regions that are not well covered by ozonesondes, the main limitation being the lack of vertical information within the troposphere.

   Some care must be taken to allow a meaningful comparison between OMI-MLS TOC and the corresponding modeled quantity (Ziemke et al., 2006). The monthly climatology of the tropopause height used within the OMI-MLS algorithm

(NCEP model, Ziemke et al. (2011)) has been also employed here to compute tropospheric columns for all the modelling experiments. This was done after the vertical interpolation of modeled O_3 fields on a common vertical pressure grid, which has been chosen identical to that available for the CAMSRA database. This approach minimises potential TOC discrepancies due to different tropopause computation or due to different vertical resolutions among models. Monthly TOC fields have been first computed for each model and then averaged temporally to compute TOC maps the four different seasons (DJF, MAM, JJA, SON), displayed in Fig. 1, 2, 3 and 4 respectively.

During DJF months (Fig. 1) the global TOC is the lowest (28.6 DU for OMI-MLS retrievals). IASI-r, IASI-a and CAMSRA show slightly higher TOC values than OMI-MLS but rather similar geographical distribution to OMI-MLS and among each other. The GEOS-CCM model shows larger TOC maxima and lower minima with respect to the other models and OMI-MLS. The MOCAGE control simulation shows less pronounced zonal variability than all other models, which is expected due to the missing tropospheric chemistry description. The visible zonal structures in the control simulation are mostly a result of the zonal variability of the tropopause height.

An increase of TOC is observed in the Northern Hemisphere (NH) mid-latitudes during MAM months (Fig. 2). Values of TOC larger than 40 DU are observed with OMI-MLS over populated continental regions as well as over oceans. Larger TOC values are predicted by CAMSRA and GEOS-CCM compared to MOCAGE based simulations and OMI-MLS. Due to the small sensitivity of IASI IR observations to the boundary layer O_3, IASI-r and IASI-a share the same limitations of the control simulation, i.e. a relaxation toward a zonal O_3 climatology in the lowermost model layers that is negatively biased (Emili et al., 2014). Such biases do affect the TOC computation to a limited extent. Nevertheless, IASI-r provides slightly larger TOC values than IASI-a, which seems more coherent with full-chemistry models and ozonesondes (Fig. 3 of the original manuscript). The decrease of TOC in the SH during the MAM months is reproduced by all models.

During JJA period (Fig. 3) values of TOC reach the maximum in the NH mid-latitudes with local maxima in the Mediterranean region, South East Asia and China. As noted previously, GEOS-CCM tends to provide larger TOC variability and extrema. IASI-r and CAMSRA provide the best match to OMI-MLS measurements in this period of the year, whereas IASI-a and the control simulation underestimate the TOC. The increase of TOC in the SH tropical and mid-latitudes with respect to MAM period is reproduced by all models except for the control simulation.

In SON months (Fig. 4) the TOC decreases significantly in the NH but increases in the SH, with a well known local maximum stretching from the South Indian Ocean to the Atlantic Ocean (Liu et al., 2017). IASI-r, CAMSRA and, in a lesser extent IASI-a, provide TOC distributions that match quite well with OMI-MLS measurements. GEOS-CCM simulates a smaller SH maximum and too large TOC values in the NH mid-latitudes. On the other end, the MOCAGE control simulation underestimates TOC values at all latitudes and does not reproduce the expected regional variability.

We remark finally that both IASI-r and IASI-a slightly overestimate TOC values inside the tropical deep convergence zone in South East Asia. This behaviour is observed for all periods of the year.

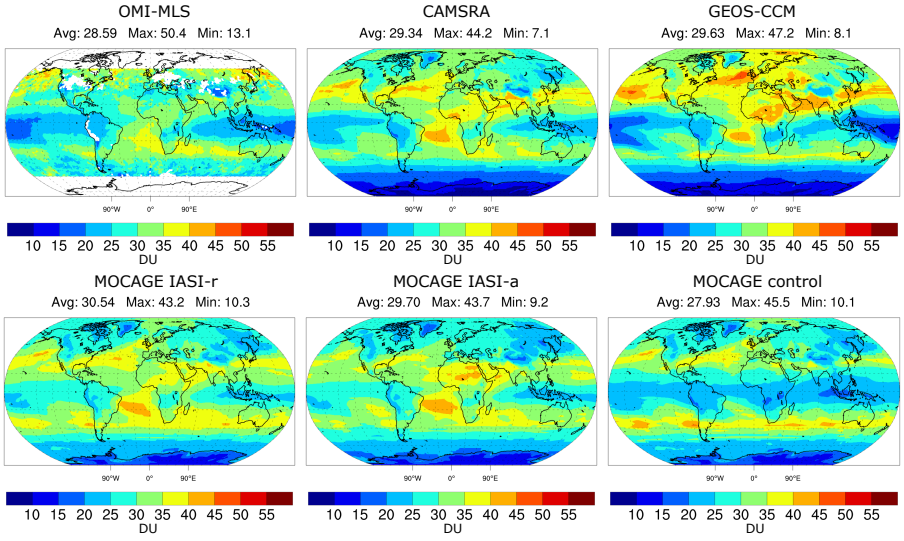

Figure 1. Tropospheric Ozone Column averaged on December-January-February 2010 from: OMI-MLS retrievals (top left), CAMSRA reanalysis (top middle), GEOS-CCM simulation (top right), IASI-r reanalysis (bottom left), IASI-a reanalysis (bottom middle) and MOCAGE control simulation (bottom right). Mean, minimum and maximum values of ozone (in DU) are depicted over each plot.

Overall IASI-r and CAMSRA TOC values are the closest to OMI-MLS measurements, both in terms of regional variability and amplitude, and for most of 2010. IASI-a TOC shows similar global patterns to IASI-r but with reduced amplitude, as anticipated from the previous section (Fig. 3 of the original manuscript).

2. *In Figure 5, in addition to showing the results of IASI-r, why not also present plots for the IASI-a product for reference?*

Answer:

The IASI-a plots were omitted because IASI-a was already validated against ozone-sondes and found to be less accurate than IASI-r (Sec. 5.1 of the original manuscript). This choice was also taken to reduce the figure's size and improve its readability. Following the comment of the reviewer, we decided to include IASI-a plots (see Fig. 5) so that all simulations are now displayed in the model vertical inter-comparison section. The following text has been added in the manuscript to comment IASI-a plots:

IASI-a results are reported for completeness (Fig. 5, third column) and their comparison with IASI-r (second column) confirms the previous findings (Sec. 5.1): IASI-r reduced significantly the tropospheric biases of IASI-a at mid and high-latitudes both in the SH and NH. Absolute differences between IASI-r/IASI-a and CAMSRA remain instead of the same order (10%) in the tropics but differ in sign as a function of the altitude and the month.

3. *Can the authors comment on the differences in computational costs for the L1 and L2 assimilation configurations, and discuss the reasons for differences, and potential means to improve on this? Also, it's good to put these differences*

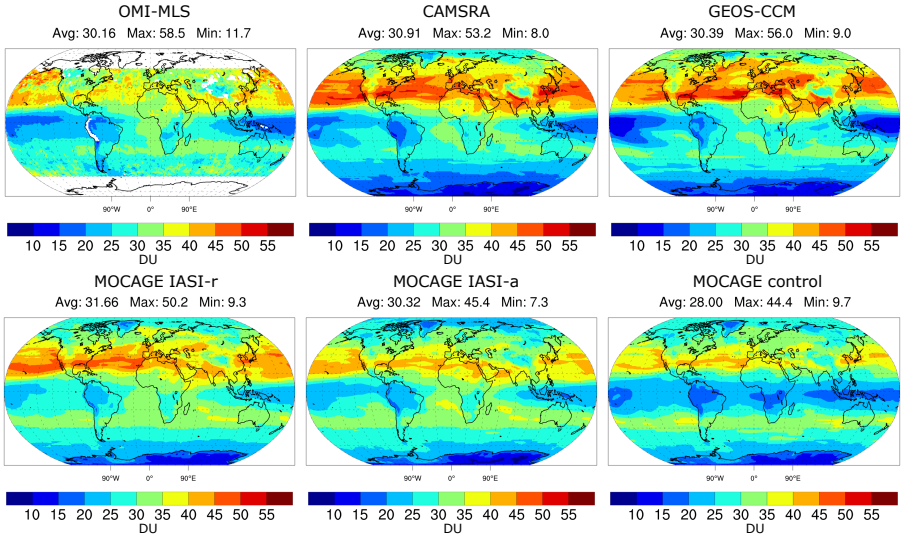

Figure 2. Tropospheric Ozone Column averaged on March-April-May 2010 from: OMI-MLS retrievals (top left), CAMSRA reanalysis (top middle), GEOS-CCM simulation (top right), IASI-r reanalysis (bottom left), IASI-a reanalysis (bottom middle) and MOCAGE control simulation (bottom right). Mean, minimum and maximum values of ozone (in DU) are depicted over each plot.

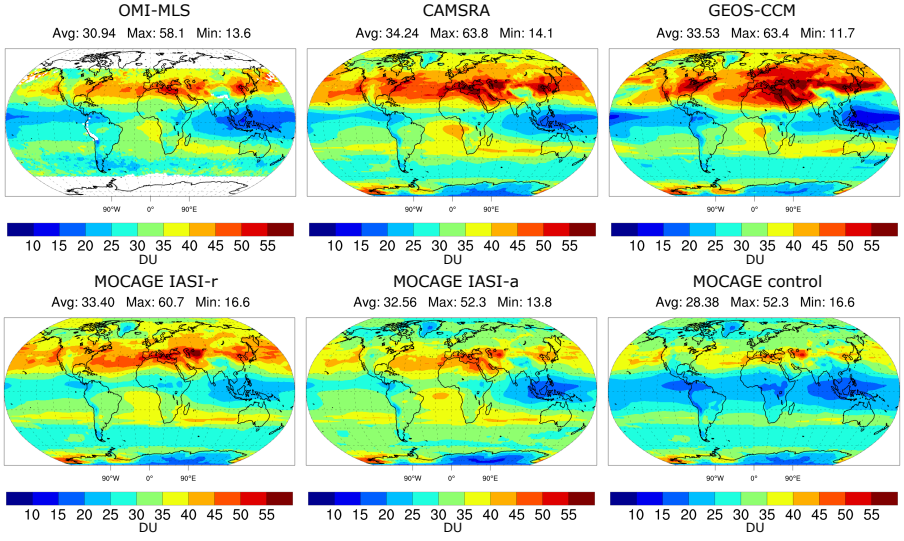

Figure 3. Tropospheric Ozone Column averaged on June-July-August 2010 from: OMI-MLS retrievals (top left), CAMSRA reanalysis (top middle), GEOS-CCM simulation (top right), IASI-r reanalysis (bottom left), IASI-a reanalysis (bottom middle) and MOCAGE control simulation (bottom right). Mean, minimum and maximum values of ozone (in DU) are depicted over each plot.

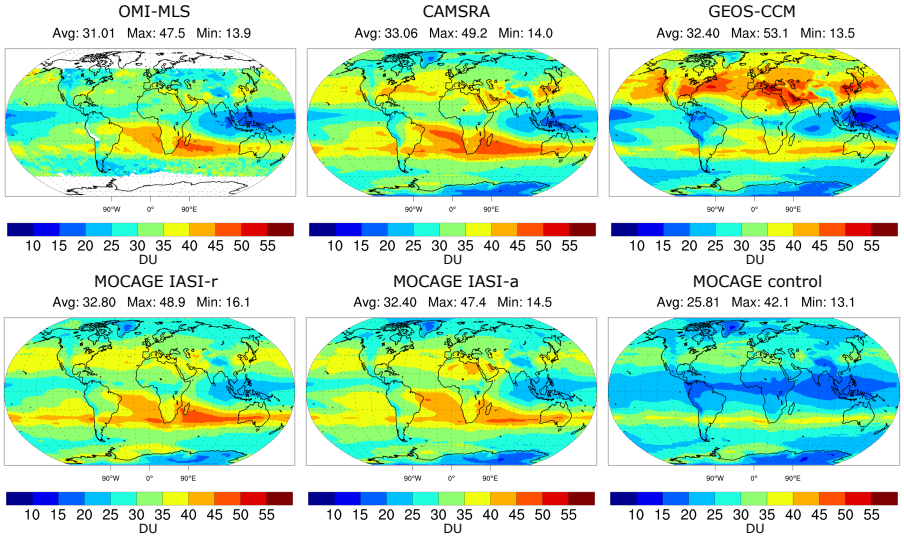

Figure 4. Tropospheric Ozone Column averaged on September-October-November 2010 from: OMI-MLS retrievals (top left), CAMSRA reanalysis (top middle), GEOS-CCM simulation (top right), IASI-r reanalysis (bottom left), IASI-a reanalysis (bottom middle) and MOCAGE control simulation (bottom right). Mean, minimum and maximum values of ozone (in DU) are depicted over each plot.

in costs into perspective, particularly in regard to their comment in the conclusion in the case "IR measurements are already assimilated", (p12, l16)

Answer: A first analysis of the difference in computational cost between L1 and L2 assimilation was given in Emili et al. (2019) Sec. 4.2. The numerical cost of assimilating L1 data is of course larger than for L2 (by a factor of 3.5 in the former study). However, the former analysis only compared the cost of the 3D-Var assimilation itself, without counting the numerical cost of the L2 retrievals. L2 retrievals also involve Radiative Transfer Model (RTM) computations and, in the particular case of the 1D-Var retrievals assimilated in IASI-a, multiple calls to the linearised and adjoint RTM are also performed during the minimisation. Considering the contribution of L2 retrievals in the overall cost will reduce significantly the differences between the two approaches. For a given number of satellite observations and using the same RTM code for both L1 assimilation and L2 retrievals (RTTOV in our case), the computational difference between the 'L2 retrieval plus assimilation' and 'L1 assimilation' can only arise from the number of iterations needed to reach convergence. The number of needed iterations for L2 retrievals and L1 assimilation depends on many factors (choice of the minimiser, scene/pixel, other assimilated instruments etc.) and it is fine tuned for each application. In general, a larger number of iterations of the minimiser is needed to find 3D or 4D-Var solutions with respect to a collection of 1D retrievals solutions. For example, about 30 iterations are needed in average for IASI L1 + MLS L2 3D-Var assimilation (IASI-r). Hence we expect that L1 assimilation might remain overall more expensive than L2 retrievals plus assimilation. A precise quantification of this overhead would require computing again the L2 retrievals with the same version of the

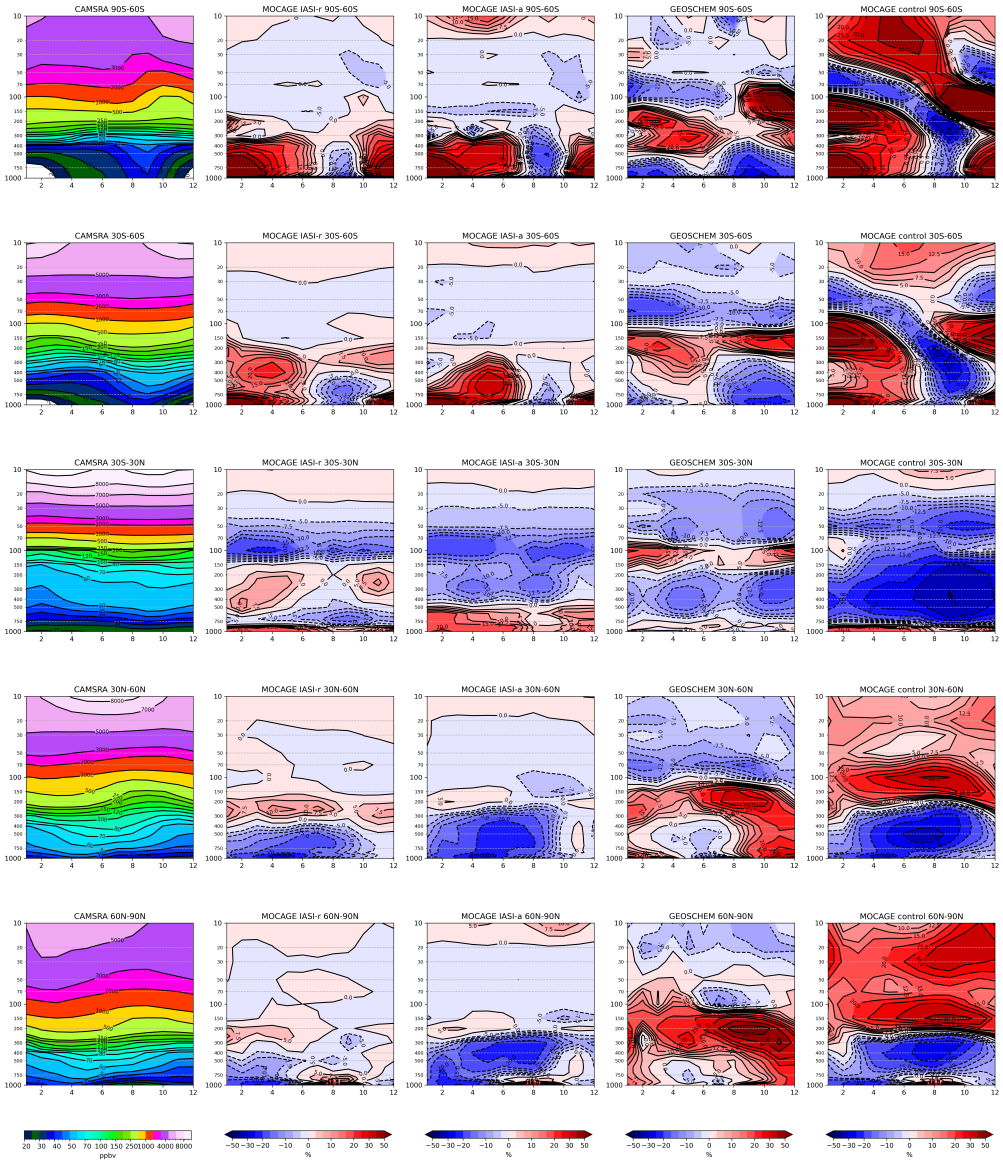

Figure 5. Ozone zonal averages as a function of month (x-axis) and altitude (y-axis in hPa) for five latitude bands separately (90°S-60°S, 60°S-30°S, 30°S-30°N, 30°N-60°N, 60°N-90°N from top to bottom). CAMSRA O_3 (in ppbv) is plotted on the first column. The relative differences between IASI-r (second column), IASI-a (third column), GEOS-CCM (fourth column), MOCAGE control simulation (fifth column) and CAMSRA O_3 are given in percent of the CAMSRA O_3.

RTM used in this study (RTTOV 11) and on the same CPUs of the L1 assimilation. This would demand a significant amount of work. However, it can be argued that this overhead would become of lesser importance when some O_3 IR

channels are already used for NWP (Dragani and Mcnally, 2013). In this case only the cost of including additional O_3 channels has to be considered. Moreover, we used until now the same IASI channel selection of Barret et al. (2011) for L1 assimilation, which seem to provide some redundant information. Ongoing studies are focused on the reduction of needed channels in the O_3 band, which represent the most straightforward way to reduce the computational cost of L1 assimilation (and L2 retrievals as well).

Since this discussion is quite technical and the experiments needed to give a precise quantification of the computational overhead of L1 assimilation cannot be done easily we prefer not to include it in the revised manuscript. However, we added the following text in the conclusions (p12, l16) to elaborate a bit further:

The additional cost of the RTM computations would in this case scale linearly with the number of added O_3 sensitive channels. In this work we used the original spectral selection of Barret et al. (2011) but the presence of strong inter-channel error correlations (Aabaribaoune et al., 2020) suggests the possibility to reduce significantly the number of assimilated channels without degrading the analysis. This represents an interesting area for further research.

4. *Furthermore, considering the data-thinning approach (pp 7, line 3), in the current study only a single observation is used in every 2x2 grid box. Can the authors explain a bit more about their data-thinning approach, e.g. do you make any additional check on selecting representative observations (apart from the dynamic filter)?*

Answer: The data thinning is performed as follows in practice: we used a regular grid of 1°×1° resolution and select the first pixel that falls in every two grid boxes. This ensures a minimum distance of 1° among assimilated observations. No additional criteria have been used to screen observations based on representativeness because it is not straightforward to define such criteria in the radiance space. We think that increasing the model resolution in the future constitutes the best way to exploit the large number of IASI observations.

The following sentence has been added in the revised manuscript for sake of clarity:

Data thinning is performed using a regular grid of 1°×1° resolution and selecting the first pixel that falls in every two grid boxes. This ensures a minimum distance of 1° among assimilated observations.

2 Reply to specific comments

Answer:

All specific comments have been integrated in the revised manuscript.

References

Aabaribaoune, M. E., Emili, E., and Guidard, V.: Estimation of the error covariance matrix for IASI radiances and its impact on ozone analyses, Atmospheric Measurement Techniques Discussions, 2020, 1–26, https://doi.org/10.5194/amt-2020-179, https://amt.copernicus.org/preprints/amt-2020-179/, 2020.

Barret, B., Le Flochmoen, E., Sauvage, B., Pavelin, E., Matricardi, M., and Cammas, J. P.: The detection of post-monsoon tropospheric ozone variability over south Asia using IASI data, Atmospheric Chemistry and Physics, 11, 9533–9548, https://doi.org/10.5194/acp-11-9533-2011, http://www.atmos-chem-phys.net/11/9533/2011/, 2011.

Dragani, R. and Mcnally, A. P.: Operational assimilation of ozone-sensitive infrared radiances at ECMWF, Quarterly Journal of the Royal Meteorological Society, 139, 2068–2080, https://doi.org/10.1002/qj.2106, 2013.

Emili, E., Barret, B., Massart, S., Le Flochmoen, E., Piacentini, a., El Amraoui, L., Pannekoucke, O., and Cariolle, D.: Combined assimilation of IASI and MLS observations to constrain tropospheric and stratospheric ozone in a global chemical transport model, Atmospheric Chemistry and Physics, 14, 177–198, https://doi.org/10.5194/acp-14-177-2014, http://www.atmos-chem-phys.net/14/177/2014/, 2014.

Emili, E., Barret, B., Le Flochmoën, E., and Cariolle, D.: Comparison between the assimilation of IASI Level 2 ozone retrievals and Level 1 radiances in a chemical transport model, Atmospheric Measurement Techniques, 12, 3963–3984, https://doi.org/10.5194/amt-12-3963-2019, https://www.atmos-meas-tech.net/12/3963/2019/, 2019.

Liu, J., Rodriguez, J. M., Steenrod, S. D., Douglass, A. R., Logan, J. A., Olsen, M. A., Wargan, K., and Ziemke, J. R.: Causes of interannual variability over the southern hemispheric tropospheric ozone maximum, Atmospheric Chemistry and Physics, 17, 3279–3299, https://doi.org/10.5194/acp-17-3279-2017, https://acp.copernicus.org/articles/17/3279/2017/, 2017.

Ziemke, J. R., Chandra, S., Duncan, B. N., Froidevaux, L., Bhartia, P. K., Levelt, P. F., and Waters, J. W.: Tropospheric ozone determined from Aura OMI and MLS: Evaluation of measurements and comparison with the Global Modeling Initiative's Chemical Transport Model, Journal of Geophysical Research, 111, D19 303, https://doi.org/10.1029/2006JD007089, http://dx.doi.org/10.1029/2006JD007089, 2006.

Ziemke, J. R., Chandra, S., Labow, G. J., Bhartia, P. K., Froidevaux, L., and Witte, J. C.: A global climatology of tropospheric and stratospheric ozone derived from Aura OMI and MLS measurements, Atmospheric Chemistry and Physics, 11, 9237–9251, https://doi.org/10.5194/acp-11-9237-2011, http://www.atmos-chem-phys.net/11/9237/2011/, 2011.